Identifying Meat from Grazing or Feedlot Yaks Using Visible and Near-infrared Spectroscopy with Chemometrics

Yuchao Liu, Yang Xiang, Wu Sun, Allan Degen, Huan Xu, Yayu Huang, Rongzhen Zhong, Lizhuang Hao

▶ **To cite this version:**

Yuchao Liu, Yang Xiang, Wu Sun, Allan Degen, Huan Xu, et al.. Identifying Meat from Grazing or Feedlot Yaks Using Visible and Near-infrared Spectroscopy with Chemometrics. Journal of Food Protection, 2024, 87 (7), pp.100295. 10.1016/j.jfp.2024.100295 . hal-04631294

HAL Id: hal-04631294
https://hal.inrae.fr/hal-04631294

Submitted on 2 Jul 2024

HAL is a multi-disciplinary open access archive for the deposit and dissemination of scientific research documents, whether they are published or not. The documents may come from teaching and research institutions in France or abroad, or from public or private research centers.

L'archive ouverte pluridisciplinaire **HAL**, est destinée au dépôt et à la diffusion de documents scientifiques de niveau recherche, publiés ou non, émanant des établissements d'enseignement et de recherche français ou étrangers, des laboratoires publics ou privés.

Distributed under a Creative Commons Attribution - NonCommercial - NoDerivatives 4.0 International License

Journal of Food Protection 87 (2024) 100295

Contents lists available at ScienceDirect

Journal of Food Protection

journal homepage: www.elsevier.com/locate/jfp

Research Paper

Identifying Meat from Grazing or Feedlot Yaks Using Visible and Near-infrared Spectroscopy with Chemometrics

Yuchao Liu [1,2], Yang Xiang [1,*], Wu Sun [1], Allan Degen [3], Huan Xu [1], Yayu Huang [4], Rongzhen Zhong [5], Lizhuang Hao [1,*]

[1] Qinghai University, Key Laboratory of Plateau Grazing Animal Nutrition and Feed Science of Qinghai Province, Xining 810016, China
[2] Qinghai Light Industry Research Institute Co., Ltd., Xining 810016, China
[3] Desert Animal Adaptations and Husbandry, Wyler Department of Dryland Agriculture, Blaustein Institutes for Desert Research, Ben-Gurion University of the Negev, Beer Sheva 8410500, Israel
[4] GenPhySE, Université de Toulouse, INRAE, INPT, ENVT, Castanet Tolosan, France
[5] Jilin Province Feed Processing and Ruminant Precision Breeding Cross Regional Cooperation Technology Innovation Center, Jilin Provincial Laboratory of Grassland Farming, State Key Laboratory of Black Soils Conservation and Utilization, Northeast Institute of Geography and Agroecology, Chinese Academy of Sciences, Changchun 130102, China

ARTICLE INFO

Keywords:
Farming system
Partial least squares discriminant analysis (PLS-DA)
Product traceability
Quality of yak meat
Soft independent modeling of class analogies (SIMCA)

ABSTRACT

The quality of meat can differ between grazing and feedlot yaks. The present study examined whether spectral fingerprints by visible and near-infrared (Vis-NIR) spectroscopy and chemo-metrics could be employed to identify the meat of grazing and feedlot yaks. Thirty-six 3.5 − year − old castrated male yaks (164 ± 8.38 kg) were divided into grazing and feedlot yaks. After 5 months on treatment, liveweight, carcass weight, and dressing percentage were greater in the feedlot than in grazing yaks. The grazing yaks had greater protein content but lesser fat content than feedlot yaks. Principal component analysis (PCA) was able to identify the meat of the two groups to a great extent. Using either partial least squares discriminant analysis (PLS-DA) or the soft independent modeling of class analogies (SIMCA) classification, the meat could be differentiated between the groups. Both the original and processed spectral data had a high discrimination percentage, especially the PLS-DA classification algorithm, with 100% discrimination in the 400–2500 nm band. The spectral preprocessing methods can improve the discrimination percentage, especially for the SIMCA classification. It was concluded that the method can be employed to identify meat from grazing or feedlot yaks. The unerring consistency across different wavelengths and data treatments highlights the model's robustness and the potential use of NIR spectroscopy combined with chemometric techniques for meat classification. PLS-DA's accurate classification model is crucial for the unique evaluation of yak meat in the meat industry, ensuring product traceability and meeting consumer expectations for the authenticity and quality of yak meat raised in different ways.

The yak (*Poephagus grunniens*) is a unique ruminant animal residing in the high-altitude regions of the Tibetan Plateau. It represents the largest grazing cattle population globally and is exceptionally adapted to the harsh environment of the Tibetan Plateau, characterized by extreme cold, low oxygen levels in the air, intense radiation, and wind, as well as a brief grass-growing season. (Jia et al., 2021; Jing et al., 2022; Liu. 2018). The yak is distributed predominantly in Qinghai, Tibet, Gansu, Sichuan, Xinjiang, and Yunnan provinces of China, accounting for approximately 95% of the world population (Ma et al., 2013; Zhang et al., 2015; Zhang et al., 2020). This bovine species is not only a vital resource for the livelihood of local residents, providing meat, milk, yak down, wool, leather, and dung but also a symbol of cultural heritage and economic asset. Therefore, it is referred to as the “Ecological Yak,” “Environmental Yak,” “Nutritional Yak,” and “Cultural Yak.” (Jing et al., 2022; Ren et al., 2022). Currently, China's annual total production of yak meat is approximately over 400,000 tons (300,000–500,000 tons) (National Technical System for Beef and Yak Industry, 2021; National Technical System

Abbreviations: VFA, volatile fatty acid; TMR, total mixer ration; SNV, standard normalized variate; R^2, coefficient of determination; RMSEC, root mean square error of correction; RMSECV, root mean square error of cross-validation; PLSR, partial least squares; PLS-DA, Partial least squares discriminant analysis; SIMCA, Soft Independent Modeling of Class Analogies.

* Corresponding authors.
E-mail addresses: chaorenxy@163.com (Y. Xiang), lizhuanghao1122@foxmail.com (L. Hao).

https://doi.org/10.1016/j.jfp.2024.100295
Received 9 February 2024; Accepted 2 May 2024
Available online 08 May 2024
0362-028X/© 2024 The Author(s). Published by Elsevier Inc. on behalf of International Association for Food Protection.
This is an open access article under the CC BY-NC-ND license (http://creativecommons.org/licenses/by-nc-nd/4.0/).

for Beef and Yak Industry, 2022). Due to its unique digestive system, yaks can convert low-quality feed into high-quality protein and fat, making their meat particularly valuable (Zuo et al., 2016). It is considered a delicacy among beef varieties, typically priced more than 30% higher than regular beef and accounting for around 4% of China's beef consumption. Yak meat is considered healthy being rich in minerals, vitamins, conjugated linoleic acid, and compared with cattle, has a greater content of protein and lesser content of fat (Zuo et al., 2016; Xiong et al., 2021).

Traditionally, yaks graze on the expansive natural grasslands of the Tibetan Plateau all year round, maintaining an ecological balance and ensuring the sustainability of these fragile ecosystems. However, with the advent of intensive farming practices, there is an increasing trend of raising yaks in feedlots, primarily on grain-based diets. This shift not only affects the meat's fatty acid composition and overall nutritional profile but also impacts the sustainable practices and the traditional pastoral culture (Alfaia et al., 2009; Descalzo et al., 2005). Feedlot diets can be enriched with specific amino acids, vitamins, and minerals, ensuring a more balanced and comprehensive nutritional profile. This leads to meat with improved levels of essential nutrients, including iron, zinc, and B vitamins, which are vital for human health (Hawley et al., 2022). Additionally, feedlot feeding can improve meat quality in terms of tenderness and marbling, making it more palatable and potentially increasing its consumption. Therefore, the nutritional quality of yak meat varies depending on the feeding method, and consumers can purchase it according to their own needs and preferences.

As global consumers become more health-conscious and environmentally aware, there is a rising demand for meat products that are not only more nutritional, but that are also produced in a sustainable manner. Consumers are increasingly seeking green, organic, and functional foods with clear geographical indications, reflecting a broader trend toward ethical consumption (Prache et al., 2005). Distinguishing meat accurately between grazing and feedlot yaks thus responds to consumer demand for transparency, allowing informed choices about health, ethical considerations, and environmental impact. It also aids in preserving the cultural heritage and traditional practices associated with yak rearing, contributing to the socio-economic development of pastoral communities.

Near-infrared spectroscopy is used to obtain information on the nutritional components of animal tissues through absorption, scattering, and reflection, enabling rapid and accurate qualitative analysis of yak meat to determine the animal feeding methods. Visible-near-infrared (Vis-NIR) spectroscopy measurements are relatively easy and generally take only a few seconds, making it a convenient, low-cost, and nondestructive method (Aleixandre-Tudó et al., 2019). Because of its convenience and effectiveness, Vis-NIR spectroscopy combined with chemometrics has been used widely in food authentication and quality assessment, including the nondestructive assessment of shell egg quality and freshness, origin tracing, and in-line inspection of agro-food products under semi-industrial conditions (Shin et al., 2021; Cruz-Tirado et al., 2024; Tejerina et al., 2021; Lanza et al., 2023; Cortés et al., 2019; Jin et al., 2023; KomboloNgah et al., 2023; Goi et al., 2022; Patel et al., 2021). Huang et al. (2015) distinguished meat among pasture-raised, concentrate-fed, and concentrate − finished pasture lambs using Vis-NIR reflectance spectroscopy, and this method is being applied to yak meat. Based on these reports, it is assumed that near-infrared spectroscopy can differentiate yak meat based on varying feeding practices. To test this hypothesis, this study examined the potential of employing spectral technology combined with chemometrics to distinguish between grazing and feedlot − fed yak meat. Such a reliable method would enhance consumer trust, support sustainable practices, and promote the economic well-being of rural communities dependent on yak rearing. This approach thereby advances the quality identification and market classification of yak meat products.

Materials and Methods

Animal management

Thirty-six, 3.5 − year − old male, castrated yaks of similar body condition were divided into grazing (n = 18) and feedlot (n = 18) yaks. The feedlot yaks were kept at the fattening yak farm of Datong Fengju Breeding Professional Cooperative. The grazing yaks grazed the alpine meadow pasture of Datong County, without supplements from 07:30 to 18:00 each day during summer. The composition and nutrient content of the pasture is presented in Table 1. Drinking water for the grazing yak was available from a streamlet and from meltwater from mountains. Yaks in the feedlot were raised in a cooperative and were fed mainly corn kernels and corn silage ad libitum; feed was added twice a day (08:00 and 18:00) (see Table 2 for details on feed composition and nutrition). Drinking water was freely available from water troughs. All yaks were dewormed with oral Ivermectin prior to the study. Datong County has a highland continental climate. The average annual temperature is 4.9°C, and the annual precipitation is 523 mm, mostly in August and less in December (Wang, 2020).

Sample collection and pretreatment

After 5 months on their regimes, the yaks were fasted, but allowed water for 24 h. They were weighed (live body weight − LBW) and then slaughtered in a commercial abattoir according to industry norms. The wool, head, hooves, tail, and viscera (except kidneys) were removed and, after 30 min, were weighed for hot carcass weight (HCW). The dressing percentage was calculated from the hot carcass weight divided by the live weight and multiplied by 100. Approximately, 1 kg of the longissimus thoracis (LT) muscle between the 12th and 13th ribs was collected and stored in a vacuum bag at − 20 °C. After thawing, fat and connective tissue were removed from the surface and the muscle was cut into regular shapes of 1 cm^3, and lyophilized for 48 h. The sample was pulverized in a planetary ball mill (PM100, Retsch, Germany) for 5 min. Subsequently, it was sieved through a 40-mesh screen in preparation for analysis.

Meat composition and color

The lyophilized powder was used for the determination of moisture (method 925.040), ash (method 938.08), crude protein (CP: method 981.10), and ether extract (EE: method 935.38) contents according to AOAC (AOAC, 1995). A portable pH meter (H1 99163 N, Hanna, Bedfordshire, UK) was calibrated and used to determine the pH of the meat at 45 min and 24 h postmortem. The colorimeter (FRU WR-18, Shenzhen Wave Optoelectronics Technology Co., Ltd., Longgang, China) was calibrated with black and white reference plates before use. The meat was cut in a direction perpendicular to the muscle fibers, and lightness (L*), redness (a*), and yellowness (b*) were measured at three points on a flat cut using illuminant D65 and the 10° standard observer (CIE, 1976). The mean of the three measurements was used for all analyses.

Analysis of feed sample

Dry matter (DM, method 976.05), crude protein (CP, method 976.05, N * 6.25), and ash (method 942.05) contents of the feedlot diets were determined according to the feed analysis (AOAC, 2005). Ether extract (EE) was measured by the Soxhlet extraction (method 920.39 (AOAC, 2000)). Concentration of phosphorus was determined by the photometric method and of calcium by the atomic absorption spectrophotometric method (method 985.01). Neutral detergent fibre (NDF) concentration was assayed with heat stable α-amylase and

Table 1
Proximal composition, Calcium, Phosphorus, Gross, and Metabolizable energy of the grazed pasture

Items	June 2019	July 2019	August 2019	September 2019	October 2019
Dry Matter (%)	94.5	94.8	94.1	94.9	94.4
Ash (%)	7.13	8.94	7.01	7.72	6.03
Crude protein (%)	13.25	13.13	12.34	10.42	5.14
Crude fat (%)	2.72	2.56	2.98	2.66	2.28
Acid detergent fiber (%)	28.5	29.7	28.4	21.7	29.0
Neutral detergent fiber (%)	45.2	44.4	47.6	66.8	65.0
Ca (%)	3.08	4.01	2.15	5.12	2.47
P (%)	0.08	0.19	0.08	0.07	0.03
GE ($MJ{\cdot}kg^{-1}$)	11.63	10.29	10.07	9.51	9.51
ME ($MJ{\cdot}kg^{-1}$)	10.41	9.01	8.78	8.19	8.19

Table 2
Composition and nutrient levels of TMR (dry matter basis)

Items (g/kg)	
Wheat stalk	9.9
Corn silage	20.1
Corn kernels	35.0
Soybean	10.5
Rapeseed meal	7.0
Oat	7.0
Wheat bran	7.0
Premix	3.5
Total	100
Nutritional level (%)	
Dry Matter (DM)	79.8
Organic material	73.9
Ash	6.39
Crude protein	16.0
Crude fat	2.83
Acid detergent fiber	12.15
Neutral detergent fiber	36.1
Ca	1.87
P	0.44
GE (MJ/kg)	16.4
ME (MJ/kg)	9.67

ME (MJ/kg) = 9.236–0.213 Ash + 0.044 CP + 0.300 EE + 0.020 ADF, the Ash, CP, EE, ADF value in the formula were the values in the table divided by 10.
GE, gross energy; ME, metabolizable energy; DM, dry matter.
a. The premix provided the following per kg of diets: vitamin A 100,000–400,000 IU/kg, vitamin D 20 000–130,000 IU/kg, vitamin E ≥ 560 IU/kg, Ca 10%–30%, NaCI 10%–30%, Cu 100 mg/kg, Fe 0.2–4 g, Mn 0.5–5 g, Zn 0.5–5 g, Se 2–15 mg, I 10–100 mg, Co 2–30 mg, $H_2O \leq 10\%$.
b. ME was calculated value (Liu, 2018), while the other values were measured.

sodium sulfite and expressed inclusive of residual ash content, and acid detergent fiber (ADF) concentration was determined using fiber bags and a fiber analyzer (ANKOM 200, ANKOM, USA) following Van Soest et al. (1991). The mean of the three measurements was used for all analyses.

Elemental analysis

The detailed procedures for biochemical methods are described by references Guo et al., 2008; Sun et al., 2011; Lizhuang et al., 2019. A 0.2 g sample of yak meat, 6 mL of BV3 HNO_3, and 2 mL of BV3 H_2O_2 were placed into a polytetrafluoroethylene (PTFE) digestion tube (Mars 240/50, CEM, Mathews, NC, USA) for 35 min, with the power at 1600 W and the temperature increased gradually to 180 °C. The digested solution was diluted to 100 mL with ultra-pure water and stored in the tube before analysis by inductively coupled plasma mass spectrometry (ICP-MS; Agilent 7700x, Santa Clara, CA, USA). The operating conditions of the ICP-MS were as follows: radio frequency power at 1600 W, auxiliary gas flow rate at 1.0 L/min, peristaltic pump flow rate at 0.1 rps, nebulization chamber temperature at 2 °C, oxide indices 0.45%, and dual current indices at 1.01%. Quantification was done by the standard external method. The Environmental Calibration Standard (Part# 5183-4688; Agilent) was used as a standard solution, and the determination coefficient of standard curve was higher than 0.99. The internal standards, Ge, In, and Bi were used to ensure the instrument's stability. The samples were measured whenever the RSD of internal standards was greater than 3%.

Visible and near-infrared (Vis-NIR) spectroscopy

The samples were scanned in reflectance mode using a near-infrared spectrometer (NIR Systems, Silver Spring, MD, USA). The processed sample was loaded into the sample cup and was scanned twice to reduce photometric variability. Reflectance data were recorded at 2 nm intervals and converted to absorbance logs (1/R) for storage (Serva et al., 2023). The mean of the three measurements was used for analysis.

Data processing and multivariate analysis

Statistical analysis was processed by RStudio 4.12 (RStudio IDE, Chicago) and OriginPro 2022b (OriginLab Corporation, Northampton, MA, USA). Spectral data were processed by Unscrambler X 10.4 (Camo Software AS, Oslo, Norway).

Spectral pretreatment

In the current study, the spectral data were preprocessed for first-order derivatives, second-order derivatives (Savitzky-Golay), standard normalized variate (SNV), and their combinations. The best spectral preprocessing method was determined by comparing the accuracy and reliability of the spectral prediction models.

Exploratory analysis

Principal component analysis (PCA) is exploratory, converting multiple correlated values into a few uncorrelated composite indicators, mainly through dimensionality reduction. The information is replaced and combined with fewer indicators, which are the main components of the original multiple indicators (Lever et al., 2017). The load describes the direction of each principal component in the original X-space, and the score is a projection of the original data onto the loading vector. PCA analysis used all samples and was done in the visible (400–780 nm), NIR (780–2500 nm), and Vis-NIR (400–2500 nm) ranges.

Classification analysis

For classification analysis, the samples were divided randomly, in which 2/3 of the samples were for training (12 from each yak treatment) and 1/3 for prediction (six from each yak treatment). The raw spectral data and preprocessed spectral numbers were classified by the partial least squares-discriminant analysis (PLS-DA) and the soft independent modeling of class analogies (SIMCA), respectively.

PLS-DA is a typical linear pattern recognition technique, a discriminant analysis method based on the partial least squares (PLSR) model. The discriminant analysis generates a regression model between the spectral data and the set class features, and maximizes the separation between predefined classification levels by calculating the likelihood that each sample belongs to a classification level. This model uses a response variable delimited by 0, with −1 representing one category and +1 representing another. SIMCA first creates its own PCA model for each type of training set and then calculates the distance between the PCA model and the sample points that need to be predicted. The final decision as to where the sample class should belong is based on the distance between the model and the sample points.

Results and Discussion

Quality characteristics of yak meat with different feeding methods

The liveweight at slaughter ($P < 0.04$), carcass weight ($P < 0.001$), and dressing percentage ($P < 0.001$) were greater in the feedlot than grazing yaks (Table 3).

Protein content was greater ($P < 0.05$), but fat content was lesser ($P < 0.05$) in grazing than in feedlot yaks (Table 4), while moisture and ash contents were greater ($P < 0.001$) in grazing than feedlot yaks. Grazing yaks had greater ($P < 0.05$) concentrations of iron and calcium, feedlot yaks had greater ($P < 0.05$) concentrations of zinc, copper, and sodium, while there was no difference ($P > 0.05$) between treatments in manganese, potassium, and magnesium.

The pH of the meat was greater in the grazing than feedlot yaks at 45 min ($P < 0.03$) and 24 h ($P < 0.001$) after slaughter, while L* and a* were also greater ($P < 0.001$) in grazing than feedlot yaks, but b* did not differ ($P > 0.05$) between treatments. The muscle's pH reflects glycolysis after slaughter and affects tenderness and water-holding capacity directly (Xu et al., 2022). The higher the pH, the slower the anaerobic glycolysis of muscle glycogen, the less water exudation loss, the more stable the protein structure, and the better the meat preservation (Zhang et al., 2015). In this study, the grazing yak had lower muscle glycogen at 45 min and 24 h postmortem resulting in higher muscle pH.

Meat color is important for the consumer in selecting meat as it indicates freshness. The color is determined by the content and physicochemical state of hemoglobin and myoglobin in the muscle and is influenced by a combination of oxidation and light reflection. Myoglobin combines with oxygen to produce oxygen-containing myoglobin that turns bright red. Brown high iron myoglobin is produced by oxidation of myoglobin or oxygenated myoglobin, which affects a*, while b* is influenced by the intake of carotenoids in the diet and the content of intramuscular and intermuscular fat (Nieto et al., 2010). The L* value of meat in grazing yaks was greater ($P < 0.05$) than in feedlot yak, which may be due to the difference in moisture content of the diet. Greater L* values are accompanied by greater water content of the meat (Wang et al., 2021; Zhang et al., 2020), and the water content was greater in the grazing than in feedlot yak meat.

Visible and near-infrared (Vis-NIR) spectral profiling

In the present study, the ground meat sample was placed in a Petri dish for analysis, and the spectral data were obtained by rotating the Petri dish several times to scan the sample. Finzi et al. (2015) concluded that the use of the Petri dish provided better calibration results than optical fibers, and Serva et al. (2021) reported that the effect of the Petri dish was irrelevant in acquiring spectral data, as the effect was constant. Figure 1 presents the average absorption spectra of yak meat in the two treatments. This provides a clearer view to compare the overall absorption trends under grazing and feedlot conditions. It is evident that while the absorbance under both grazing and feedlot conditions is similar across most wavelengths, at certain wavelengths (like those mentioned previously), the samples from grazing

Table 3
Liveweight at slaughter, carcass weight, and dressing percent of grazing and feedlot yaks

Items	Grazing yaks	Feedlot yaks	SEM	*P* Values
Liveweight (kg)	229.3 ± 21.36 [a]	244.1 ± 18.62[b]	3.523	0.033
Carcass weight (kg)	101.6 ± 1.75 [a]	124.8 ± 1.90[b]	2.760	<0.001
Dressing percentage	44.0 ± 0.01 [a]	51.0± 0.01[b]	0.006	<0.001

Notes: different letters in rows with different letters are statistically significantly different ($P < 0.05$).

Table 4
Chemical and physical properties of meat from grazing and feedlot yaks

Items	Grazing	Feedlot	SEM	*P* Values
Moisture (%)	73.5 ± 1.03 [a]	71.8 ± 1.08[b]	0.23	<0.001
Ash (%)	5.72 ± 0.73 [a]	4.04 ± 0.15[b]	0.17	<0.001
Fat (g/100 g)	2.78 ± 1.40 [a]	5.62 ± 3.19[b]	0.47	0.002
Protein (g/100 g)	86.4 ± 2.64 [a]	83.3 ± 2.69[b]	0.51	<0.001
Zn (mg/100 g)	3.27 ± 0.66 [a]	4.49 ± 0.84[b]	0.16	<0.001
Fe (mg/100 g)	4.15 ± 0.41 [a]	3.63 ± 1.07[b]	0.14	0.064
Cu (mg/100 g)	0.10 ± 0.02 [a]	0.12 ± 0.03[b]	0.01	0.021
Mn (mg/100 g)	0.038 ± 0.01 [a]	0.048 ± 0.02 [a]	0.003	0.104
Ca (mg/100 g)	9.71 ± 3.40 [a]	6.83 ± 1.95[b]	0.48	0.002
K (mg/100 g)	300.8 ± 13.24 [a]	2,901 ± 36.4 [a]	4.64	0.255
Mg (mg/100 g)	33.3 ± 2.79 [a]	35.1 ± 5.01 [a]	0.71	0.216
Na (mg/100 g)	58.6 ± 5.27 [a]	77.6 ± 20.23[b]	2.96	0.001
pH_{45min}	6.97 ± 0.12 [a]	6.85 ± 0.16[b]	0.02	0.023
pH_{24h}	5.62 ± 0.17 [a]	5.43 ± 0.10[b]	0.03	<0.001
L*	32.4 ± 3.44 [a]	30.8 ± 1.69[b]	0.46	<0.001
a*	15.1 ± 2.15 [a]	11.9 ± 2.31[b]	0.45	<0.001
b*	13.9 ± 2.16 [a]	14.9 ± 1.38 [a]	0.31	0.096

Notes: different letters in rows with different letters are statistically significantly different ($P < 0.05$).

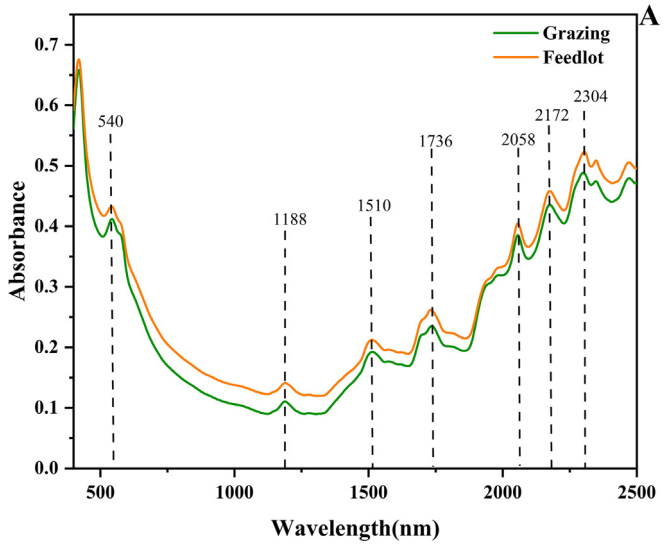

Figure 1. Average of absorption spectra.

yaks exhibit a slightly higher ability to absorb light than those from feedlot yaks.

The spectral and feed data analyses distinctly underscore the quality and compositional variations between yak meat from grazing and feedlot systems, especially within specific wavelength ranges. In Figure 1, the original and average near-infrared (NIR) spectral data from yak meat samples revealed absorption peaks within key wavelength ranges that were associated with various constituents such as proteins, fats, and moisture. Among them, absorption peaks at 540 nm, 1188 nm, and 1510 nm are related to moisture, representing the combination frequency absorption band of O–H groups. Absorption peaks at 1736 nm and 2304 nm are related to fat, representing the first harmonic absorption of C–H groups and the combination frequency absorption of stretching and bending vibrations of C–H groups, respectively. Absorption peaks at 2058 nm and 2172 nm are related to protein, representing the harmonic and combination frequency vibrations of N–H groups (Yan et al., 2005). Particularly, differences in absorption intensities at certain NIR wavelength ranges, typically between 700 nm and 2500 nm, are indicative of variations in diet source, fatty acid composition, and moisture content—factors critical to assessing meat quality (Goi et al., 2022). The feed data for grazing yaks (Table 1) displayed large seasonal fluctuations in nutrients like crude protein and total energy, impacting the meat's nutritional quality and taste. Conversely, feedlot yaks (Table 2) received a controlled and nutritionally balanced diet, leading to higher overall nutritional value. The NIR spectroscopy effectively captured these variations, with specific wavelength ranges being particularly telling of the feeding regime's influence on the meat's quality. Employing this spectral analysis within these defined wavelength ranges is pivotal for discerning the subtle differences in yak meat quality, guiding improvements in rearing practices. Moreover, the high absorption peaks at 430 nm and 500 nm were associated with respiratory and carotenoid pigments stored in fat (Cozzolino & Murray, 2002; Ripoll et al., 2015). Moreover, it was reported that β-Carotene was greater in the muscle of grazing than in feedlot yaks (Li et al., 2015).

Exploratory analysis

The structure and content of fat, protein, water, and other components in yak meat can differ due to dietary intake. Therefore, the position, peak, and intensity of absorption peaks in the NIR spectra differed between treatments. To identify the essential spectral changes that distinguish the two yak groups, the spectra of the 36 samples were analyzed by PCA.

The first two principal components were used as inputs for the classification model because too many variables reduce the computational speed and cover most of the information while maintaining the interpretability of PCA (Song et al., 2021; Zhang et al., 2020). The cumulative contribution of the first two principal components in all three cases was greater than 95%, representing most of the information in the original spectrum, and explaining most of the information in the original data (Fig. 2A–C). The first two principal components separated the meat between the two yak groups; the feedlot yaks were mainly on the positive side of PC2, while the grazing yaks were mainly on the negative side of PC2. Consequently, it was possible to distinguish between yak groups based on spectral curve reflectance values.

The loading diagram and the scoring diagram can complement each other's descriptions. Loads of PC1 and PC2 are presented in Figure 2D. Absorption peaks were observed at 430 and 500 nm associated with carotenoids. Since carotenoids are fat-soluble, the wavelengths at which C–H bonds absorb infrared energy may also be relevant to their absorption (Barragán et al., 2021). Animals cannot synthesize carotenoids, so these pigments may play an essential role in differentiating groups of animals due to dietary intake (Barragán et al., 2021). In addition, there was a substantial difference in CIELAB color space (Fig. 1). Negative loads were observed at 1190 and 1940 nm, which were associated with water, where the 1190 nm absorption peak indicated the secondary multiplicative absorption of C–H (Yan et al., 2005). The effect of water in freeze-dried samples should be minor but is also associated with the first and second overtones of protein changes, and the C–H and N–H stretch in the combinatorial bands (Barbin et al., 2015). This was observed at 1694 nm associated with fatty acid C–H bond, and at 1520, 2060, and 2180 nm associated with proteins (Yan et al., 2005). The absorption peaks at 2060 and 2180 nm indicated the absorption bands of protein amides, and the peak at 2060 nm was due to the N–H stretching vibration (Yan et al., 2005). As these proteins vary due to differences in dietary intake, the different strengths of these bands most likely are responsible for the differences determined by the Vis-NIRS technique in this study.

Chemometrics analysis

To distinguish the meat between the two yak groups, a Vis-NIR spectroscopy model was generated by comparing different wavelengths of NIR spectra and combining two pattern recognition methods, PLS-DA and SIMCA, to measure the suitability of the samples and the identification model based on the correct discrimination rate. In optical nondestructive testing, some noise is inevitable in the acquired spectral information due to interference from internal and external factors by the optical detection system. Appropriate spectral preprocessing can eliminate interference from baseline drift, noise, light scattering, and sample inhomogeneities, while optimizing spectral information and improving the accuracy and robustness of the model. The derivative process improves the resolution of the spectra and reduces the interference of baseline drift and background noise. The data set was divided into two parts: 24 samples were used as a training set to construct the prediction models, and the best preprocessing method was selected according to the three indices of the calibration model, i.e., coefficient of determination (R^2), root mean square error of correction (RMSEC), and root mean square error of cross-validation (RMSECV). The larger the R^2 and the smaller the RMSEC and RMSEP indicated greater the accuracy of the model. The best preprocessing method was the SNV, first-order derivative (five points) + SNV, and second-order derivative (five points) + SNV in the 400–780 nm spectrum, 780–2500 nm spectrum, and 400–2500 nm spectrum, respectively (Table 5). Then, the remaining 12 samples were used to assess the accuracy of the prediction models.

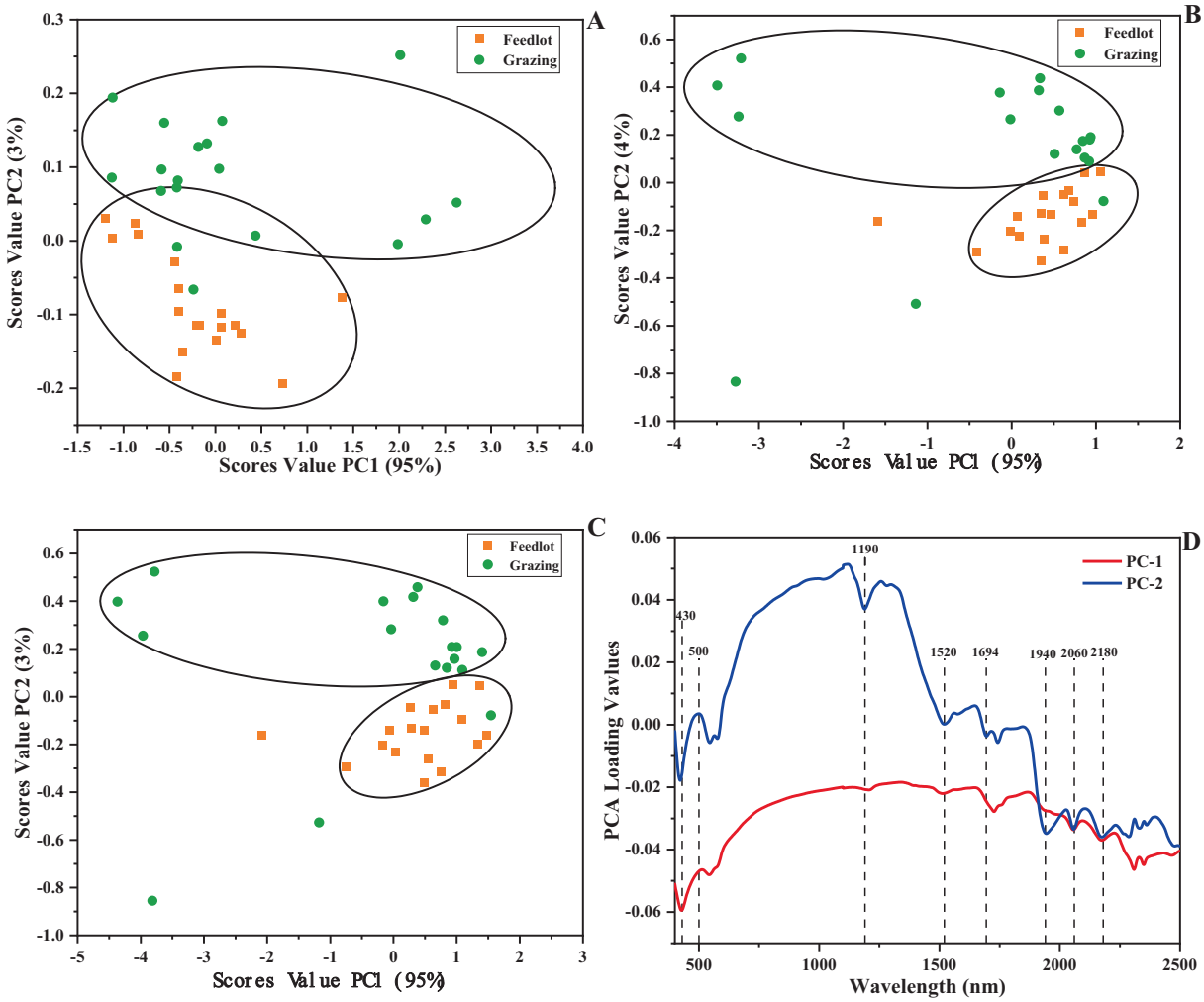

Figure 2. Score values (A, B, C) obtained from PCA of the spectra in wavelength ranges: 400–780 nm, 780–2500 nm, and 400–2500 nm, and loadings (D) obtained from PCA of the spectra in wavelength ranges: 400–2500 nm.

Table 5
The parameters of partial least squares discriminant analysis (PLS-DA) calibration models using different preprocessing methods

Range	Preprocessing	R^2	RMSEC	RMSECV
400–780 nm	Original	0.870	0.361	0.521
	Standard normalized variate (SNV)	0.967	0.182	0.347
	First-order derivative (5 points) + SNV	0.829	0.414	0.590
	Second-order derivative (5 points) + SNV	0.795	0.452	0.724
780–2500 nm	Original	0.844	0.395	0.738
	Standard normalized variate (SNV)	0.705	0.544	0.724
	First-order derivative (5 points) + SNV	0.975	0.159	0.478
	Second-order derivative (5 points) + SNV	0.958	0.206	0.429
400–2500 nm	Original	0.861	0.373	0.548
	Standard normalized variate (SNV)	0.893	0.327	0.465
	First-order derivative (5 points) + SNV	0.904	0.310	0.480
	Second-order derivative (5 points) + SNV	0.989	0.103	0.449

The establishment of the discriminant model is presented in Figure 3 and Figures s2. The provided image features six confusion matrices labeled A through F, which display the results of a discriminant analysis-partial least squares-discriminant analysis (PLS-DA)-applied to near-infrared spectroscopy data for classifying the meat samples as either from grazing or feedlot yaks. Matrices A to C depict classifications using raw spectral data across the wavelength ranges of 400–780 nm, 780–2500 nm, and 400–2500 nm, respectively. Matrices D to F mirror this setup but with preprocessed spectral data. Remarkably, all matrices show perfect classification with zero misclassifications, as the off-diagonal quadrants—which would indicate false negatives and false positives—are all zero. This suggests that the PLS-DA model is exceptionally accurate across all examined spectral ranges, with either raw or preprocessed data.

The discrimination rate of the preprocessed spectral data by the SIMCA model was distinctly higher than that of the original spectral

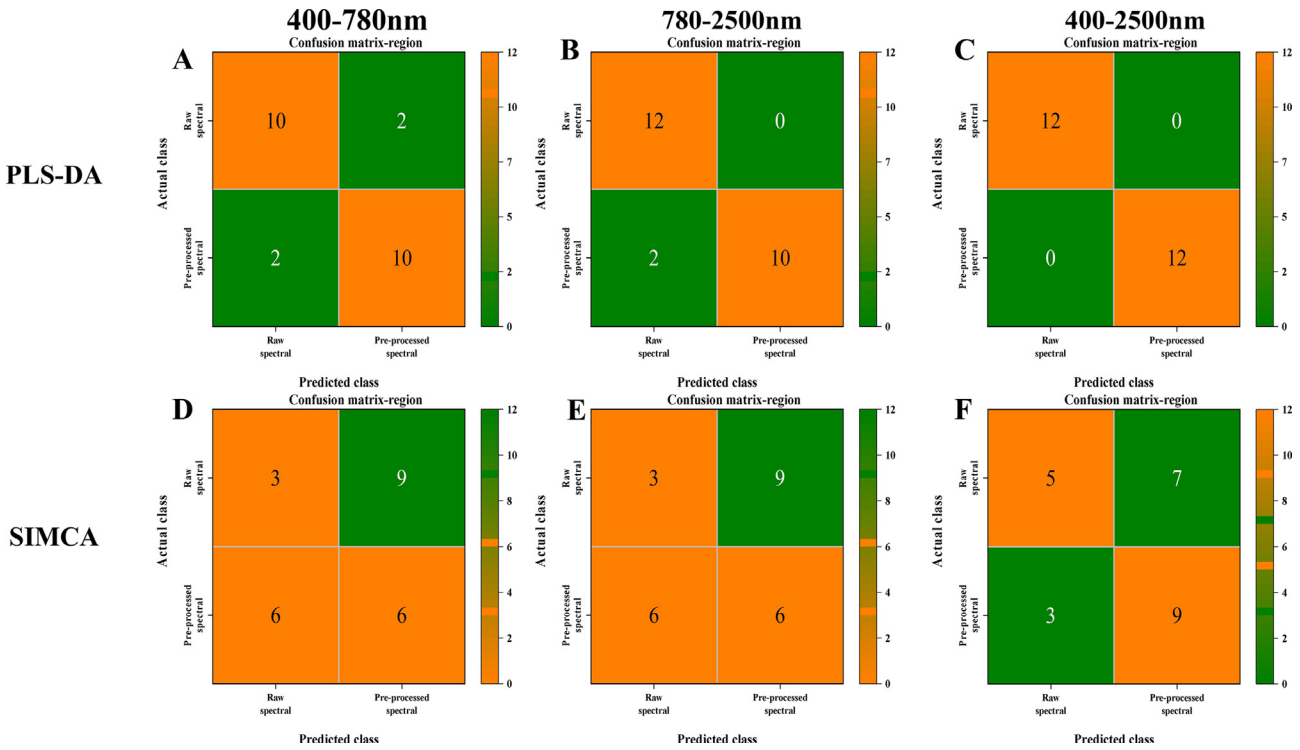

Figure 3. The plots (A-C) display the reclassification of the test samples in total by using the constructed PLS-DA model, and validate the discriminant ability of the model in the 400–780 nm, 780–2500 nm, and 400–250 nm wavelength ranges; The plots (D-F) display the reclassification of the test samples in total by using the constructed SIMCA model, and validate the discriminant ability of the model in the 400–780 nm, 780–2500, nm and 400–250 nm wavelength ranges.

data because SIMCA is a supervised pattern recognition method based on PCA. The core idea was to describe the training set by building a separate PCA model for each sample classification. On this basis, the classification of the unknown sample can be predicted by fitting the principal component model of each classification in turn. Preprocessing the spectral data improved the accuracy of the PCA submodel of each classification in the training set. The confusion matrices labeled H to M represent the classification of meat samples using the SIMCA model across various NIR spectral ranges, revealing the discriminant capabilities of the model. The matrices corresponding to the raw spectral data (H, I, and J) demonstrated that the model achieved very strong classification in the 780–2500 nm range (I), but was weaker in the narrower 400–780 nm range (H) and the full 400–2500 nm range (J). Interestingly, the preprocessed spectral data (K, L, and M) exhibited a notable improvement in classification accuracy. In particular, matrix M, which included the full spectral range, achieved flawless classification with no misclassifications, suggesting that preprocessing techniques such as normalization or baseline correction may enhance the SIMCA model's predictive accuracy considerably by reducing spectral noise and highlighting distinguishing features. Comparing the two supervised modeling methods, PLS-DA and SIMCA, it was clear that the discrimination rate of PLS-DA was slightly better, which was in agreement with a previous study (Firmani et al., 2019).

In the PLS-DA matrices (A-C), the classification was impeccable for the broader wavelength ranges (780–2500 nm and 400–2500 nm) with no observed misclassifications, suggesting a robust model performance. However, some misclassifications were noted in the narrower range (400–780 nm). In contrast, the SIMCA matrices (D-F) revealed misclassifications across all wavelength ranges, indicating a comparative reduction in accuracy. This analysis emphasizes the superior discriminant power of the PLS-DA model, particularly in the combined wavelength range of 400–2500 nm, and highlights potential areas for improvement in the SIMCA model. Accurate classification models like PLS-DA are vital for the meat industry, ensuring product traceability and meeting consumer expectations for authenticity and quality. The 400–780 nm band had a relatively low discrimination rate in both models, probably due to the low information on the contained components, mainly carotenoids, which can also be seen in Figure 3. However, Serrano et al. (2007) suggested that carotenoid pigments are suitable biomarkers for grazing herbivores, which is slightly inconsistent with the results of this study. The carotenoid content in adipose tissue may be higher than that in muscle tissue, or it may differ among animal species. Further studies are warranted on yak fat.

The current study revealed a strong accuracy of meat classification across different wavelengths and data treatments of NIR spectroscopy combined with chemometric techniques. Such reliable differentiation is vital for quality control and authentication in the meat industry, ensuring product integrity and consumer trust. The feasibility of using NIR spectroscopy to differentiate meat from yaks raised under different feeding systems was demonstrated, but some problems still need to be solved. For example, both breed and interannual variation can affect the content or structure of the chemical components of yak meat. The VIS-NIR of meat from different parts of yaks should be tested. However, this study examined a feasible and highly accurate method for distinguishing meat between grazing and feedlot yaks. Consequently, VIS-NIR can be an effective tool which not only helps to determine the authenticity of labels but also ensures the food safety and integrity of yak meat. Additionally, this method can provide useful insights to food technology professionals and students specializing in food safety, laying a foundation for understanding traceability in meat products in subsequent studies.

Conclusion

This study determined the differences in meat quality between grazing and feedlot yaks and utilized visible and near-infrared (Vis-NIR) spectroscopy fingerprinting and chemometrics to distinguish

the meat between the two groups of yaks. In meat, protein content was greater and fat content was lesser in grazing than in feedlot yaks. The combination of Vis-NIR with partial least squares discriminant analysis (PLS-DA) or soft independent modeling of class analogies (SIMCA) classification effectively differentiated meat between grazing and feedlot yaks. The consistent accuracy across different wavelengths and data processing highlighted the robustness of the model, with the discrimination rate in the 400–2500 nm range surpassing that of the 400–780 nm and 780–2500 nm ranges. The selection of spectral preprocessing methods can enhance resolution, particularly with SIMCA classification. An accurate PLS-DA classification model is crucial for the meat industry, as it enables product traceability and provides consumers with authenticity and quality measures.

CRediT authorship contribution statement

Yuchao Liu: Writing – original draft. **Yang Xiang:** Writing – review & editing, Methodology. **Wu Sun:** Resources. **Allan Degen:** Validation, Investigation. **Huan Xu:** Resources. **Yayu Huang:** Data curation. **Rongzhen Zhong:** Formal analysis. **Lizhuang Hao:** Methodology, Funding acquisition.

Declaration of competing interest

The authors declare that they have no known competing financial interests or personal relationships that could have appeared to influence the work reported in this paper.

Acknowledgment

The authors give thanks for the financial support received from the National Key Research and Development Sub-project “Qinghai Yak and Tibetan Sheep Adaptive Variety Selection and Efficient Breeding Technology Integration Demonstration” (2022YFD1302103); Provincial Key Laboratory Incentive Funds-Key Laboratory of Plateau Grazing Animal Nutrition and Feed Science of Qinghai Province (2024).

Appendix A. Supplementary material

Supplementary data to this article can be found online at https://doi.org/10.1016/j.jfp.2024.100295.

References

Alfaia, C. P. M., Alves, S. P., Martins, S. I. V., Costa, A. S. H., Fontes, C. M. G. A., Lemos, J. P. C., Bessa, R. J. B., & Prates, J. A. M. (2009). Effect of the feeding system on intramuscular fatty acids and conjugated linoleic acid isomers of beef cattle, with emphasis on their nutritional value and discriminatory ability. *Food Chemistry, 114* (3), 939–946. https://doi.org/10.1016/j.foodchem.2008.10.041.

Aleixandre-Tudó, J. L., Castelló-Cogollos, L., Aleixandre, J. L., & Aleixandre-Benavent, R. (2019). Bibliometric insights into the spectroscopy research field: A food science and technology case study. *Applied Spectroscopy Reviews, 55*(9–10), 873–906. https://doi.org/10.1080/05704928.2019.1694936.

AOAC (1995). *Official Methods of Analysis* (16th ed.). Washington, D.C., USA: Association of Official Analytical Chemists.

AOAC (2005). *Official methods of analysis of AOAC international* (18th ed.). Gaithersburg, MD: Association of Official International.

AOAC (2000). *Official Methods of Analysis of the Association of Official Analytical Chemists International* (17th ed.). Arlington, VA, USA: AOAC International.

Barragán, W., Aalhus, J. L., Penner, G., Dugan, M. E. R., Juárez, M., López-Campos, Ó., Vahmani, P., Segura, J., Angulo, J., & Prieto, N. (2021). Authentication of barley-finished beef using visible and near infrared spectroscopy (Vis-NIRS) and different discrimination approaches. *Meat Science, 172*. https://doi.org/10.1016/j.meatsci.2020.108342.

Barbin, D. F., Kaminishikawahara, C. M., Soares, A. L., Mizubuti, I. Y., Grespan, M., Shimokomaki, M., & Hirooka, E. Y. (2015). Prediction of chicken quality attributes by near infrared spectroscopy. *Food Chemistry, 168*, 554–560. https://doi.org/10.1016/j.foodchem.2014.07.101.

Cruz-Tirado, J. P., Vieira, M. S. S., Correa, O. O. V., Delgado, D. R., Angulo-Tisoc, J. M., Barbin, D. F., & Siche, R. (2024). Detection of adulteration of Alpaca (Vicugna pacos) meat using a portable NIR spectrometer and NIR-hyperspectral imaging. *Journal of Food Composition and Analysis, 126*. https://doi.org/10.1016/J.JFCA.2023.105901.

Cortés, V., Blasco, J., Aleixos, N., Cubero, S., & Talens, P. (2019). Monitoring strategies for quality control of agricultural products using visible and near-infrared spectroscopy: A review. *Trends in Food Science & Technology, 85*, 138–148. https://doi.org/10.1016/j.tifs.2019.01.015.

Cozzolino, D., & Murray, I. (2002). Effect of sample presentation and animal muscle species on the analysis of meat by near infrared reflectance spectroscopy. *Journal of Near Infrared Spectroscopy, 10*(1), 37–44. https://doi.org/10.1255/jnirs.319.

Descalzo, A. M., Insani, E. M., Biolatto, A., Sancho, A. M., Garcia, P. T., Pensel, N. A., & Josifovich, J. A. (2005). Influence of pasture or grain-based diets supplemented with vitamin E on antioxidant/oxidative balance of Argentine beef. *Meat Science, 70*(1), 35–44. https://doi.org/10.1016/j.meatsci.2004.11.018.

Finzi, A., Oberti, R., Negri, A. S., Perazzolo, F., Cocolo, G., Tambone, F., Cabassi, G., & Provolo, G. (2015). Effects of measurement technique and sample preparation on NIR spectroscopy analysis of livestock slurry and digestates. *Biosystems Engineering, 134*, 42–54. https://doi.org/10.1016/j.biosystemseng.2015.03.015.

Firmani, P., De Luca, S., Bucci, R., Marini, F., & Biancolillo, A. (2019). Near infrared (NIR) spectroscopy-based classification for the authentication of Darjeeling black tea. *Food Control, 100*, 292–299. https://doi.org/10.1016/j.foodcont.2019.02.006.

Goi, A., Hocquette, J.-F., Pellattiero, E., & De Marchi, M. (2022). Handheld near-infrared spectrometer allows on-line prediction of beef quality traits. *Meat Science, 184*. https://doi.org/10.1016/j.meatsci.2021.108694.

Guo, B. L., Wei, Y. M., Pan, J. R., & Li, Y. (2008). Stable C and N isotope ratio analysis for regional geographical traceability of cattle in China. *Food Chemistry, 118*(4), 915–920. https://doi.org/10.1016/j.foodchem.2008.09.062.

Hawley, A. L., Liang, X., Børsheim, E., Wolfe, R. R., Salisbury, L., Hendy, E., Wu, H., Walker, S., Tacinelli, A. M., & Baum, J. I. (2022). The potential role of beef and nutrients found in beef on outcomes of wellbeing in healthy adults 50 years of age and older: A systematic review of randomized controlled trials. *Meat Science, 189*. https://doi.org/10.1016/J.MEATSCI.2022.108830.

Huang, Y., Andueza, D., de Oliveira, L., Zawadzki, F., & Prache, S. (2015). Comparison of visible and near infrared reflectance spectroscopy on fat to authenticate dietary history of lambs. *Animal, 9*(11), 1912–1920. https://doi.org/10.1017/s1751731115001172.

Jia, J., Liang, C., Wu, X., Xiong, L., Bao, P., Chen, Q., & Yan, P. (2021). Effect of high proportion concentrate dietary on Ashdan Yak jejunal barrier and microbial function in cold season. *Research in Veterinary Science, 140*, 259–267. https://doi.org/10.1016/j.rvsc.2021.09.010.

Jing, X., Ding, L., Zhou, J., Huang, X., Degen, A., & Long, R. (2022). The adaptive strategies of yaks to live in the Asian highlands. *Animal Nutrition, 9*, 249–258. https://doi.org/10.1016/j.aninu.2022.02.002.

Jin, P., Fu, Y., Niu, R., Zhang, Q., Zhang, M., Li, Z., & Zhang, X. (2023). Non-destructive detection of the freshness of air-modified mutton based on near-infrared spectroscopy. *Foods, 12*(14). https://doi.org/10.3390/foods12142756.

KomboloNgah, M., Goi, A., Santinello, M., Rampado, N., Atanassova, S., Liu, J., Faure, P., Thoumy, L., Neveu, A., Andueza, D., De Marchi, M., & Hocquette, J.-F. (2023). Across countries implementation of handheld near-infrared spectrometer for the on-line prediction of beef marbling in slaughterhouse. *Meat Science, 200*. https://doi.org/10.1016/j.meatsci.2023.109169.

Liu, H. L. (2018). *Prediction and evaluation of effective energy in feeds of yak. Master's Thesis*. Xining: Qinghai University.

Lanza, I., Currò, S., Segato, S., Serva, L., Cullere, M., Catellani, P., Fasolato, L., Pasotto, D., & Dalle, Z. A. (2023). Spectroscopic methods and machine learning modelling to differentiate table eggs from quails fed with different inclusion levels of silkworm meal. *Food Control, 147*. https://doi.org/10.1016/j.foodcont.2022.109589.

Lizhuang, H., Yang, X., Huang, Y., Hocquette, J. F., & Liu, S. (2019). Using mineral elements to authenticate the geographical origin of yak meat. *Kafkas Universitesi Veteriner Fakultesi Dergisi, 25*, 93–98. https://doi.org/10.9775/kvfd.2018.20366.

Lever, J., Krzywinski, M., & Altman, N. (2017). Principal component analysis. *Nature Methods, 641–642*. https://doi.org/10.1038/nmeth.4346.

Li, Y., Carrillo, J. A., Ding, Y., He, Y., Zhao, C., Liu, J., Liu, G. E., Zan, L., & Song, J. (2015). Transcriptomic profiling of spleen in grass-fed and grain-fed Angus cattle. *PLOS ONE, 10*(9), e0135670. https://doi.org/10.1371/journal.pone.0135670.

Ma, Z. J., Zhong, J. C., Han, J. L., Xu, J. T., Liu, Z. N., & Bai, W. L. (2013). Research progress on molecular genetic diversity of the yak (Bos grunniens). *Yi Chuan, 35*(2), 151–160.

National Technical System for Beef and Yak Industry. (2021). Technical Development Report on Beef and Yak Industry, Ministry of Agriculture – National Technical System for Beef and Yak Industry.

National Technical System for Beef and Yak Industry. (2022). Technical Development Report on Beef and Yak Industry, Ministry of Agriculture – National Technical System for Beef and Yak Industry.

Prache, S., Cornu, A., Berdagué, J. L., & Priolo, A. (2005). Traceability of animal feeding diet in the meat and milk of small ruminants. *Small Ruminant Research, 59*(2–3), 157–168. https://doi.org/10.1016/j.smallrumres.2005.05.004.

Patel, N., Toledo-Alvarado, H., & Bittante, G. (2021). Performance of different portable and hand-held near-infrared spectrometers for predicting beef composition and quality characteristics in the abattoir without meat sampling. *Meat Science, 178*. https://doi.org/10.1016/j.meatsci.2021.108518.

Ren, W., Huang, C., Ma, X., La, Y., Chu, M., Guo, X., Wu, X., Yan, P., & Liang, C. (2022). Association of HSF1 gene copy number variation with growth traits in the Ashidan yak. *Gene, 842*, 146798. https://doi.org/10.1016/j.gene.2022.146798.

Ripoll, G., Casasús, I., Joy, M., Molino, F., & Blanco, M. (2015). Fat color and reflectance spectra to evaluate the β-carotene, lutein and α-tocopherol in the plasma of bovines finished on meadows or on a dry total mixed ration. *Animal Feed Science and Technology, 207*, 20–30. https://doi.org/10.1016/j.anifeedsci.2015.05.014.

Shin, S., Lee, Y., Kim, S., Choi, S., Kim, J. G., & Lee, K. (2021). Rapid and non-destructive spectroscopic method for classifying beef freshness using a deep spectral network fused with myoglobin information. *Food Chemistry, 352*. https://doi.org/10.1016/J.FOODCHEM.2021.129329.

Soest, P. J. V., Robertson, J. B., & Lewis, B. A. (1991). Methods for dietary fiber, neutral detergent fiber and non-starch polysaccharides in relation to animal nutrition. *Journal of Dairy Science, 74*, 3583–3597. https://doi.org/10.3168/jds.s0022-0302(91)78551-2.

Sun, S., Guo, B., Wei, Y., & Fan, M. (2011). Multi-element analysis for determining the geographical origin of mutton from different regions of China. *Food Chemistry, 124*(3), 1151–1156. https://doi.org/10.1016/j.foodchem.2010.07.027.

Serva, L., Marchesini, G., Cullere, M., Ricci, R., & Dalle Zotte, A. (2023). Testing two NIRs instruments to predict chicken breast meat quality and exploiting machine learning approaches to discriminate among genotypes and presence of myopathies. *Food Control, 144*. https://doi.org/10.1016/j.foodcont.2022.109391.

Serva, L., Marchesini, G., Chinello, M., Contiero, B., Tenti, S., Mirisola, M., Grandis, D., & Andrighetto, I. (2021). Use of near-infrared spectroscopy and multivariate approach for estimating silage fermentation quality from freshly harvested maize. *Italian Journal of Animal Science, 20*(1), 859–871. https://doi.org/10.1080/1828051x.2021.1918028.

Song, J., Shao, Y., Yan, Y., Li, X., Peng, J., & Guo, L. (2021). Characterization of volatile profiles of three colored quinoas based on GC-IMS and PCA. *LWT - Food Science and Technology, 146*. https://doi.org/10.1016/j.lwt.2021.111292.

Serrano, E., Prache, S., Chauveau-Duriot, B., Agabriel, J., & Micol, D. (2007). Traceability of grass-feeding in young beef using carotenoid pigments in plasma and adipose tissue. *Animal Science, 82*(6), 909–918. https://doi.org/10.1017/ASC200698.

Tejerina, D., Contador, R., & Ortiz, A. (2021). Near infrared spectroscopy (NIRS) as tool for classification into official commercial categories and shelf-life storage times of pre-sliced modified atmosphere packaged Iberian dry-cured loin. *Food Chemistry, 356*. https://doi.org/10.1016/j.foodchem.2021.129733.

Wang (2020). Study on Water Consumption Characteristics of Typical Forests in Loess Alpine Region. *Datong County, Qinhai Province. Master's Thesis*. Beijing: Beijing Forestry University.

Wang, B., Li, H., Huang, Z., Kong, B., Liu, Q., Wang, H., Xu, M., & Xia, X. (2021). Dynamic changes in the qualities and heterocyclic aromatic amines of roasted pork induced by frying temperature and time. *Meat Science, 176*, 108457. https://doi.org/10.1016/j.meatsci.2021.108457.

Xiong, L., Pei, J., Kalwar, Q., Wu, X., Yan, P., & Guo, X. (2021). Fat deposition in yak during different phenological seasons. *Livestock Science, 251*. https://doi.org/10.1016/j.livsci.2021.104671.

Xu, M., Chen, X., Huang, Z., Chen, D., Li, M., He, J., Chen, H., Zheng, P., Yu, J., Luo, Y., & Yu, B. (2022). Effects of dietary grape seed proanthocyanidin extract supplementation on meat quality, muscle fiber characteristics and antioxidant capacity of finishing pigs. *Food Chemistry, 367*, 130781. https://doi.org/10.1016/j.foodchem.2021.130781.

Yan, Y., Zhao, L., Han, D., & Yang, S. (2005). *Fundamentals and applications of near infrared spectroscopy analysis* (pp. 350–353). CHN: Light Industry Press.

Zhang, L., Sun, B., Xie, P., Li, H., Su, H., Sha, K., Huang, C., Lei, Y., Liu, X., & Wang, H. (2015). Using near infrared spectroscopy to predict the physical traits of Bos grunniens meat. *LWT – Food Science and Technology, 64*(2), 602–608. https://doi.org/10.1016/j.lwt.2015.06.022.

Zhang, Q., Degen, A., Hao, L., Huang, Y., Niu, J., Wang, X., Chai, S., & Liu, S. (2020). An increase in dietary lipid content from different forms of double-low rapeseed reduces enteric methane emission in Datong yaks on the Qinghai-Tibetan Plateau. *Animal Science Journal, 91*(1), e13489. https://doi.org/10.1111/asj.13489.

Zuo, H., Han, L., Yu, Q., Niu, K., Zhao, S., & Shi, H. (2016). Proteome changes on water-holding capacity of yak longissimus lumborum during postmortem aging. *Meat Science, 121*, 409–419. https://doi.org/10.1016/j.meatsci.2016.07.010.

Zhang, C., Luo, J., Yu, B., Zheng, P., Huang, Z., Mao, X., He, J., Yu, J., Chen, J., & Chen, D. (2015). Dietary resveratrol supplementation improves meat quality of finishing pigs through changing muscle fiber characteristics and antioxidative status. *Meat Science, 102*, 15–21. https://doi.org/10.1016/j.meatsci.2014.11.014.

Nieto, G., Diaz, P., Banon, S., & Garrido, M. D. (2010). Effect on lamb meat quality of including thyme (Thymus zygis ssp. gracilis) leaves in ewes' diet. *Meat Science, 85*(1), 82–88. https://doi.org/10.1016/j.meatsci.2009.12.009.

Zhang, L., Du, H., Zhang, P., Kong, B., & Liu, Q. (2020). Heterocyclic aromatic amine concentrations and quality characteristics of traditional smoked and roasted poultry products on the northern Chinese market. *Food and Chemical Toxicology, 135*, 110931. https://doi.org/10.1016/j.fct.2019.110931.

Zhang, X., He, L., Zhang, J., Whiting, M. D., Karkee, M., & Zhang, Q. (2020). Determination of key canopy paramters for mass mechanical apple harvesting using supervised machine learning and principal component analsis (PCA). *Biosystems Engineering, 193*, 247–263. https://doi.org/10.1016/j.biosystemseng.2020.03.006.